United Nations
Educational, Scientific and
Cultural Organization

IHE DELFT
Institute for
Water Education
in partnership with UNESCO

CROP TYPE MAPPING

Identify the spatial distribution of crop types from remote sensing on Google Earth Engine (GEE) – Miandoab, Iran

Fengbo Zhang
Program: HWR
Student number: 1068520
Email: Fzh001@un-ihe.org

Contents

List of Figures

List of Tables

Identify the spatial distribution of crop types from remote sensing on Google Earth Engine (GEE) – Miandoab, Iran

Zhang Fengbo
Program: HWR Student number: 1068520 Locker number: 333 Email: fzh001@un-ihe.org

1. Introduction

Lake Urmia is second-largest hypersaline lakes in the world, located in the northwest of Iran (Fig.1). However, the shrinkage of Urmia lake and the reduction of the flow into the Urmia Lake has accelerated due to uncontrolled growth of the irrigated area. Especially, a dramatic decline in lake level occurred starting in 1995(*Schulz et al.*, 2020). Thus, the new policy for Miandoad Irrigated Scheme (MIS), which is of strategic importance for food security, was proposed including reducing water allocated to MIS by 40% by increasing the performance of the scheme without compromising food production from Iran government(*Michel*, 2017). Meanwhile, Urmia Lake Restoration Program (ULRP) was established for restoring the lake. Hence to **monitor the change in the agriculture area in the Miandoab alluvial plain where is the upstream of the Urmia Lake,** the aim of this assignment **for the identification of the land cover** is necessary**.**

There are many studies that focus on the classification of the land cover estimated from the remotely sensed data (*Fang*, 1998; *Gallego*, 2004; *Lewis and Brown*, 2001; *Stehman*, 2009). Remote sensing is a technique of obtaining information about the Earth's surface with a long-distance without contact it. The recording reflected or emitted energy and analyzing the information are the based functions of RS(*Joseph*, 2005). In this case study, the analyzation of surface data acquiring from RS **for decreasing the amount of a tremendous and expensive in-situ measurement** is a convenience for classifying the land cover by GEE.

Google Earth Engine (GEE) is a cloud-based geospatial processing platform for large-scale environmental monitoring and analysis(*Tamiminia et al.*, 2020). The remote sensing imagery from the open source can be directly searched in the free-to-use GEE platform, and machine learning algorithms are calculated by Google's computational infrastructure with high speed. **For analyzing the batch images from RS, the GEE code editor based on JavaScript was used in this assignment.**

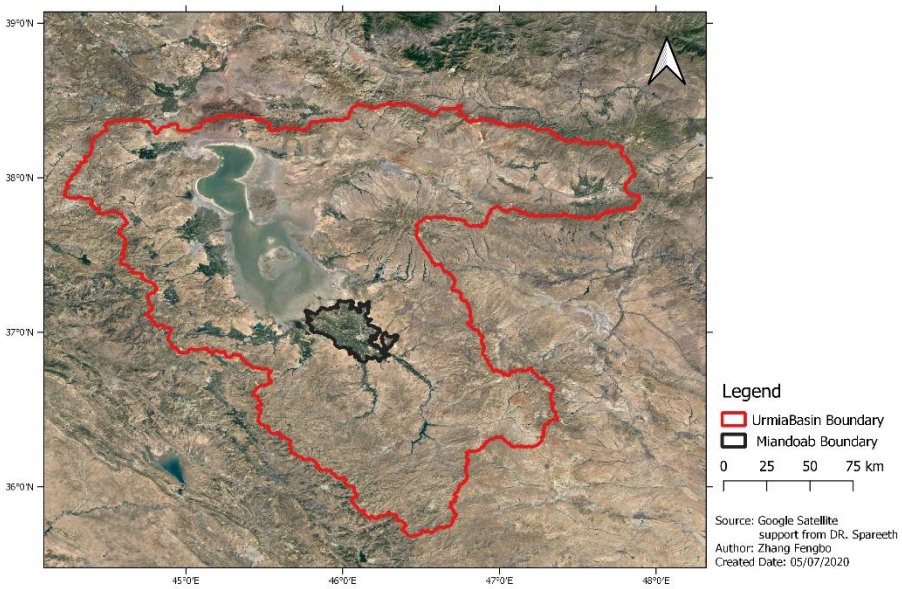

Figure 1 Boundary of Urmia Basin (red line) and Miandoab (black line)

2. Study Area

The Urmia Lake in northwest Iran is an endorheic lake and also the one of the largest hypersaline which is collected by a closed drainage basin, called Lake Urmia basin, with an area of around 51800 km2(Fig.1). However, starting in 1995, there is a strong decrease in lake level from 1278.5 m to 1271. 58 in 2012 due to multiple reasons, as shown in fig.2. *Schulz et al.* (2020) indicated that the increase of the irrigated area, accompanied by the extensive construction of the reservoir and poor agricultural water use efficiency is the main factor leading to the lake level decline. Meanwhile, the gradual reduction of precipitation in this area over time due to climate change results in decreasing the flow into the lake(*Faramarzi*, 2012).

Annual averaged evaporation and precipitation in the basin are 1150 mm and 398mm, respectively. There are around 6000 million cubic meters water discharged into the Lake Urmia contributed by thirteen rivers, including Zarrine River, which is the main river in the southeast of the Urmia basin and accounts for 50 % of the water reaching into the lake. The study area in Miandoab alluvial plain along the Zarrine River is the sub-catchment of the Urmia Lake Basin with an area of around 2322 km2(Fig. 1). It is 1,314 metres above the sea level, at 46°6'E latitude and 36°58'N longitude. The population was 135880, in 38704 families at the 2012 census. Agriculture activities in this area highly influence on the flow in the Zarrine River and the amount of groundwater seepage into the lake. Because there have illegal surface water pumps pumping form the river and tens of thousands of legal and illegal wells for groundwater extract in the catchment(*JICA*, 2016). Moreover, the demand for drink water supply to the Miandoab continuously increases due to the rise of the population(*Hesami and Amini*, 2016). Therefore, the crop type map delineated for monitoring the irrigated area is significant, providing useful information for the Iran government to devising informed strategies for water-saving.

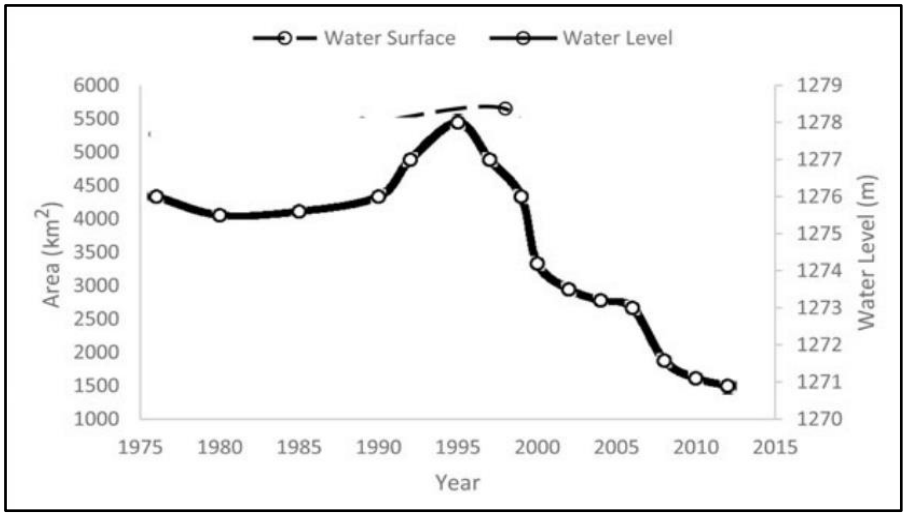

Figure 2 Changes in the water surface and water level (Hesami and Amini, 2016)

For the land cover classification, the in-situ investigation of the crop types in Miandoab is importance. Thus, the typical crop calendar is shown in fig.3, presenting that the crop year for MIS is from October to September next year, and the figure also indicates two major cropping seasons in this area. The winter cropping season is from October to June next year and summer cropping season is from May to September the same year. Major winter crops are Wheat and Barley, while summer crops are mainly vegetables and sugar beet. There are all year crops like Orchards and Alfa-Alfa. (*from the assignment's Introduction*). In this case study, the crop year selected was from October 2018 to September 2019.

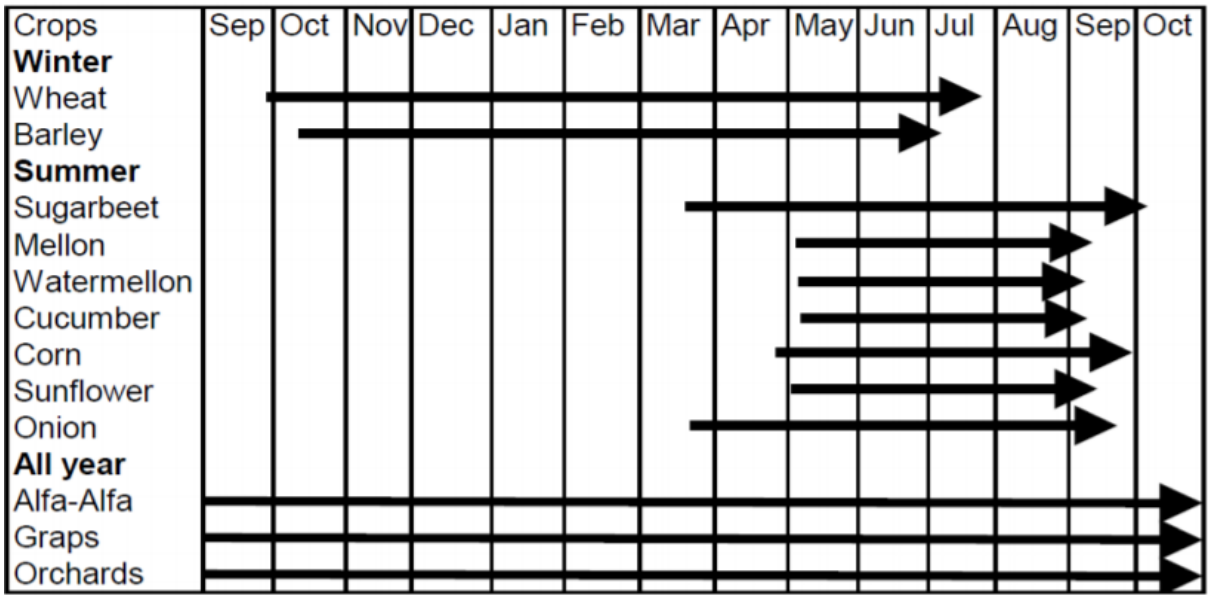

Figure 3 A typical crop calendar in Miandoab (Source: from slides in class)

3. Methodology

3.1 General workflow

The general workflow for the land cover classification is shown in fig.4. First of all, data collection in the in-situ and by RS is the first step. Field data collected in the study area should include the crop types or land use with precise coordinates. Due to the expensive consumption of in-situ measurements, ground-truth data was provided by Dr.Spareeth. Moreover, the wavelength of images, which record reflected or emitted energy from RS, are differently divided into different bands. Then, the supervised image classification is done by extracting information classes from a multiband raster image to determine the land type, like pixel datum in fig.5. There are several machine learning algorithms to achieve the goal. Random Forest and Classification And Regression Trees (CART) were used in this study. After that, the field data divide into two groups - Training and Validation - which account for 70% and 30%, respectively. The data in the training group is for Supervised Classification, and that in the validation group is for validating the accuracy. Last but not least, the crop type map should be validated and accuracy assessment is needed.

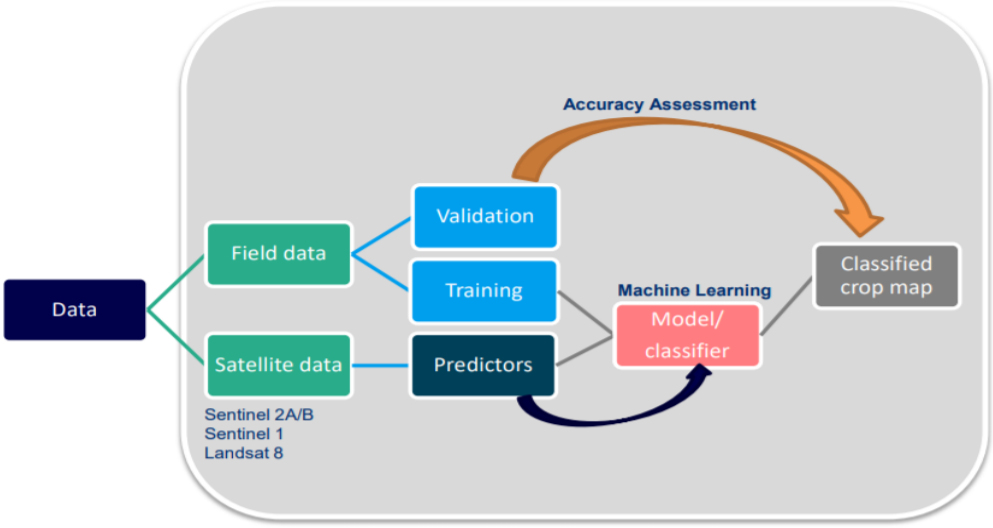

Figure 4 General workflow of the Land cover classification (Source: from slides in class)

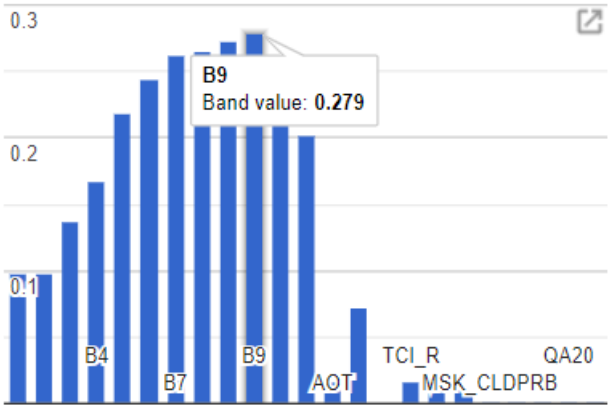

Figure 5 Pixel datum containing the multiply values from sentinel 1 and sentinel 2 at 46.1132N, 37.0296E (Source: GEE)

3.2 Introduction of Satellite products and other

Multi-date Sentinel - 1 SAR GRD and Sentinel - 2 MSI imagery were used to analyze the land cover change. Sentinel2 is a multispectral image consist of 10 bands in the visible and infrared portion of the spectrum of electromagnetic waves, as shown in fig.6. The ground spatial resolution of images is 10 m for the band 2,3,4,8 in the visible and near-infrared, and 20 m for band 5, 6, 7, 8a, 11, 12 in visible and shortwave infrared. Cirrus band 10 with 60 m pixel size was not used because of low resolution. On the other hand, Sentinel 1 is a day-and-night radar image consists of 4 bands. The advantage of the radar images is that radio waves can transmit through clouds, and the accuracy of the classification may increase by the combination with those two products.

Note that, for assessing the effect of different resolution or satellites on the accuracy of the land cover classification, the images consisting of band 2/3/4/5/6/7 in the visible and infrared from Landsat 8 Surface Reflectance Tier 1 was used, and the ground spatial resolution of images is 30 m (Fig.7).

Landsat 8 OLI			Sentinel-2 MSI		
Band	Wavelength range (nm)	Resolution (m)	Band	Wavelength range (nm)	Resolution (m)
1 Coastal aerosol	433 - 453	30	1 Coastal aerosol	433 - 453	60
2 Blue (B)	450 - 515	30	2 Blue (B)	458 - 523	10
3 Green (G)	525 - 600	30	3 Green (G)	543 - 578	10
4 Red (R)	630 - 680	30	4 Red (R)	650 - 680	10
			5 Red edge 1 (RE1)	698 - 713	20
			6 Red edge 2 (RE2)	733 - 748	20
			7 Red edge 3 (RE3)	773 - 793	20
5 Near infrared (NIR)	845 - 885	30	8 Near infrared (NIR)	785 - 900	10
			8a Near infrared narrow (NIRn)	855 - 875	20
			9 Water vapour	935 - 955	60
9 Shortwave infrared / Cirrus	1360 - 1390	30	10 Shortwave infrared / Cirrus	1360 - 1390	60
6 Shortwave infrared 1 (SWIR1)	1560 - 1660	30	11 Shortwave infrared 1 (SWIR1)	1565 - 1655	20
7 Shortwave infrared 2 (SWIR2)	2100 - 2300	30	12 Shortwave infrared 2 (SWIR2)	2100 - 2280	20
8 Panchromatic	500 - 680	15			

Figure 6 Band property in Sentinel-2 MIS and Landsat 8 OLI (Source: from slides in class)

According to the typical crop calendar, the images were divided into four groups by season per three months from October 2018 to September 2019. Moreover, the boundary of the study area was provided by Dr.Spareeth.

3.3 Machine learning algorithms for classification

Supervised Classification is the technique in which pixel values are identified with the crop type found in the pixels corresponding to the training groups(*Hesami and Amini*, 2016). And there has mang supervised machine learning algorithm to make a decision tree (fig.7) or regression tree for determining pixel values corresponding the crop type. Then, computer automatic predicts the land cover in the whole study area using the decision trees. In this assignment, Random Forest and Classification And Regression Trees (CART) were used.

Supervised machine learning algorithms is the application of artificial intelligence (AI) that can remember the data and classification in the past for predicting the unknown data(*Alpaydin*, 2020). In the beginning, the algorithm analysis the training dataset from in-situ, and then an inferred function, such as a decision tree or regression tree, is built to make predictions. The learning algorithm can also make an accuracy assessment to detect errors in modifying the model.

A decision tree is a flowchart-like structure with a series of questions, and the results are predicted by each question answers, as shown in figure 8. It can be automatically constructed by machine learning algorithms. However, the regression trees is a trend line of the training dataset in a parametric coordinate system to make predictions.

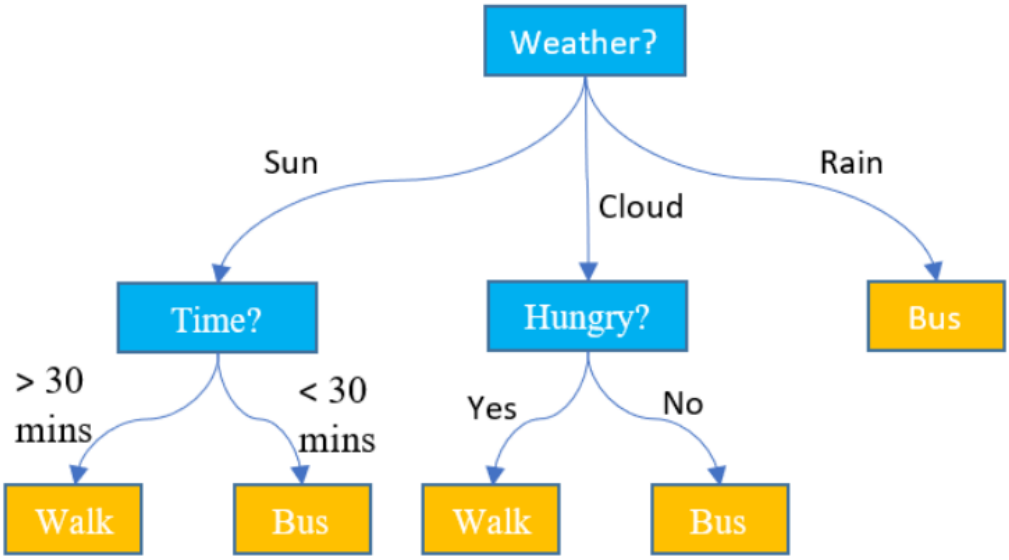

Figure 7 Example of a decision tree (Source: https://www.displayr.com/what-is-a-decision-tree/)

Random forests algorithm is one of the common supervised machine learning algorithms to create a huge number of the classification or regression trees randomly and determine the results in the best predictors. The details of the steps are posed in the paper of *Liaw and Wiener*(2002) as follows:

"*1. Draw n_{tree} bootstrap samples from the original data;*
2. For each of the bootstrap samples, grow an unpruned classification or regression tree, with the following modification: at each node, rather than choosing the best split among all predictors, randomly sample m_{try} of the predictors and choose the best split from among those variables. (Bagging can be thought of as the special case of random forests obtained when m_{try} = p, the number of predictors.);
3. Predict new data by aggregating the predictions of the n_{tree} trees (i.e., majority votes for classification, average for regression) (Liaw and Wiener, 2002)."

Due to the limitation of the assignment pages, the specific details of CART algorithm are not be introduced.

3.4 Accuracy assessment

Accuracy assessment is a process by which the accuracy or correctness of an image classification after predictions. The precision of the crop type map is calculated in the comparison of the image classification to validation dataset that is true.

Figure 8 is an example of an error matrix using three classes (*from slides in class*). Overall accuracy is the sum of the diagonals divided by the total. User's accuracy is the diagonals divided by the row sum of classification data, and the producer accuracy is that divided by the column sum of reference data

Kappa statistic is used to measure inter-rater reliability for qualitative items. A kappa of 1 indicates perfect agreement, whereas a kappa of 0 indicates agreement equivalent to chance. A limitation of kappa is that it is affected by the prevalence of the finding under observation(*McHugh*, 2012).

		Reference Data			
		Hardwood	**Conifer**	**Other**	**Total**
Classification Data	**Hardwood**	24	10	4	38
	Conifer	5	30	2	37
	Other	1	1	23	25
	Total	30	41	29	100

Figure 8 An example of error matrix (Source: from slides in class)

3.5 Scripts in GEE

The batch images process for classification achieves in GEE code editor by JavaScript. Here is my code link: https://code.earthengine.google.com/f42c8c3816a2bb36e4c7502ef2553504

The meaning of the code is explained with green sentences (start from //)

4. Results

In this assignment, Crop type map according to the Sentinel 1/2 and random forests algorithm was drawn, and the several error matrix tables were presented for the validation report.

4.1 False colour composite (FCC) images

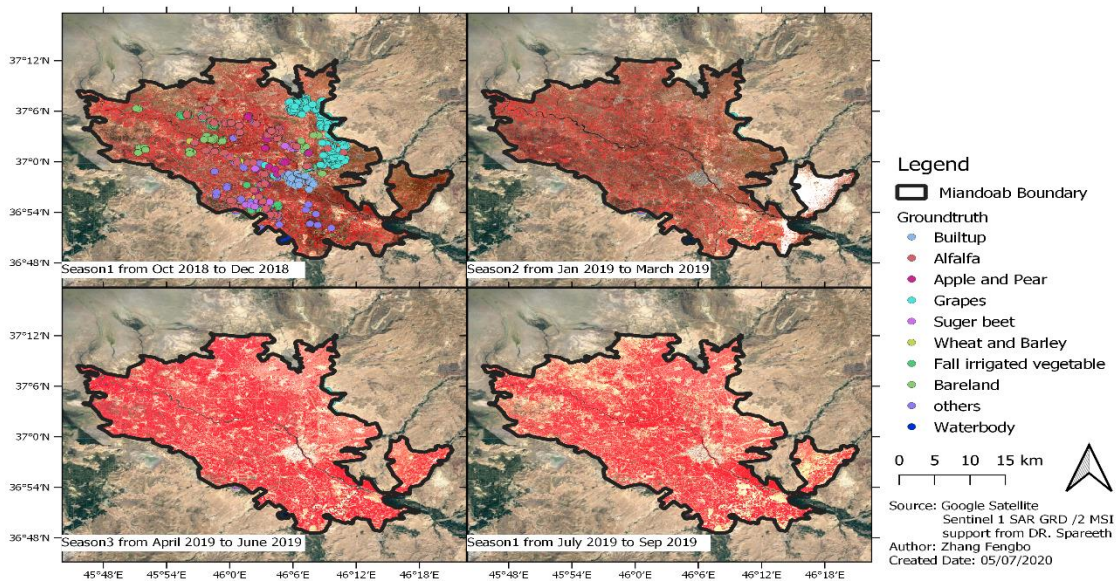

Figure 9 False Colour Composite (FCC) in four seasons from Sentinel ½ and ground-truth data (point)

Figure 9 presents the false colour composite (FCC) image in four seasons divided by the typical crop calendar for monitoring the change of the irrigated area. It is obvious that the irrigated area in season from April 2019 to September 2019 is larger than that in the previous half years, especially the season3, which have the largest irrigated area compared with other time. Because it is the overlap season of winter season and summer season, which wheat and barley were not harvested and summer crops had been planted. Moreover, the field data, which contain information about crop types or land use, were plot in the figure by different colour points. The majority of same type points are concentrated in one area, especially Builtup and Grapes, and the number of points represented water is less.

4.2 Crop type map and land area

The crop type map draws by GEE from Sentinel ½ in Miandoab is shown in fig. 10. Different colour represents different land cover or crop types. The yellow represents the Builtup with an area of 45.6 km2, and the green represents Alfalfa with an area of 222.3 km2, as shown in table 1. The area of apple and pear is 63 km2, close to the area of Others of 63.3 km2, with grey and light green respectively in the figure. Moreover, the areas of the Gapes, Wheat and Barley and Bareland apparently lager than other land covers with 216.4 km2, 210.9 km2 and 165.7 km2 respectively. They present with turquoise, dark blue and respectively in fig.10. Fall irrigated vegetable, and sugar beet is not too much in Miandoab with an area of 90.3 km2 and 25.5 km2, presenting indigo and red pixels respectively in the figure. Last but not least, it is strange that the area of Water is only 3.1 km2 which is lowest one with light blue pixels due to the false prediction to the Others in some area, indicating red arrow in the figure.

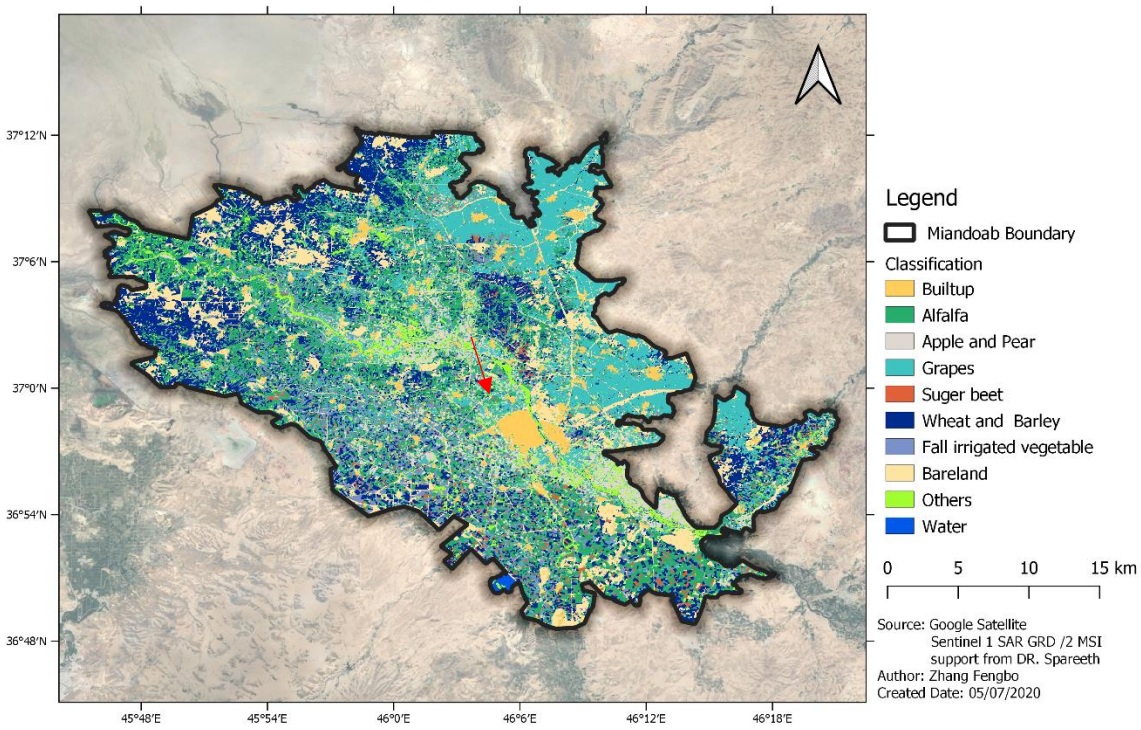

Figure 10 Crop type map from Sentinel ½

Table 1 Area of land cover classification

Class_id	Crop type	Area(km2)
1	Builtup	45.6
2	Alfalfa	222.3
3	Apple and Pear	63
4	Grapes	216.4
5	Sugar beet	25.5
6	Wheat and Barley	210.9
7	Fall irrigated vegetable	90.3
8	Bareland	165.7
9	Others	63.3
10	Water	3.1

4.3 Validation report and accuracy estimates

Table 2 Error Matrix for accuracy assessment

Class_id		Groundtruth data										
		1	2	3	4	5	6	7	8	9	10	Total
Classification data	1	14	0	0	0	0	0	0	0	0	0	14
	2	0	18	0	0	0	1	1	0	0	0	20
	3	0	3	9	0	0	1	1	0	0	0	14
	4	0	1	0	101	0	0	0	0	0	0	102
	5	0	0	0	0	10	0	4	0	0	0	14
	6	0	0	0	1	0	14	0	1	2	0	18
	7	0	0	0	2	2	1	21	0	0	0	26
	8	1	0	0	0	0	0	0	13	0	0	14
	9	0	3	3	0	1	2	4	2	15	0	30
	10	0	0	0	0	0	0	0	0	0	2	2
	Total	15	25	12	104	13	19	31	16	17	2	254

The accuracy of the crop type map was calculated by GEE automatically, as shown in table 3, and table 2 presents the error matrix by validation for accuracy assessment. The results of the land cover classification is good according to the validation report, which presents that the percentage of overall accuracy is 85% and the Kappa statistic is close to 1 with 0.85.

However, there have 15 points that falsely predict to Others area with low producer accuracy of 50 %, and points of 4 falsely predict to Apple and pear with producer accuracy of 64%. The producer accuracies of land cover, including Builtup, Alfalfa, Grapes, Bareland and Water, are higher than 90%. Moreover, the producer accuracy of Sugar beet, Wheat and Bareley and Fall irrigated vegetable remain medium positions, account for 71%, 78% and 81% respectively.

As a whole, user's accuracies are stable, compared with producer one. Most of them are above 70%, except user's accuracy in the Fall irrigated vegetable with 68%. The estimations and classifications of Water, Grapes and Builtup are good due to the user's accuracy above 90%. Other crop types remain the median positions with accuracy from 72% to 88%.

Table 3 Accuracy of crop type map

Class_id	Crop type	User's accuracy	Producer accuracy
1	Builtup	93%	100%
2	Alfalfa	72%	90%
3	Apple and Pear	75%	64%
4	Grapes	97%	99%
5	Sugar beet	77%	71%
6	Wheat and Barley	74%	78%
7	Fall irrigated vegetable	68%	81%
8	Bareland	81%	93%
9	Others	88%	50%
10	Water	100%	100%
Overall accuracy		85%	
Kappa		0.82	

4.4 Accuracy estimates with the change of the parameters

The accuracy of land cover classification may be impacted by the variation of parameters. In this assignment, images from a satellite, called Landsat 8 Surface Reflectance Tier 1 were selected for the comparison of accuracy in different satellites. Moreover, Classification and Regression Trees (CART) was used to identify land cover, and the accurate estimation of results was compared with the estimation by Random forest test for exploring the influence.

4.4.1 Effect of different RS source

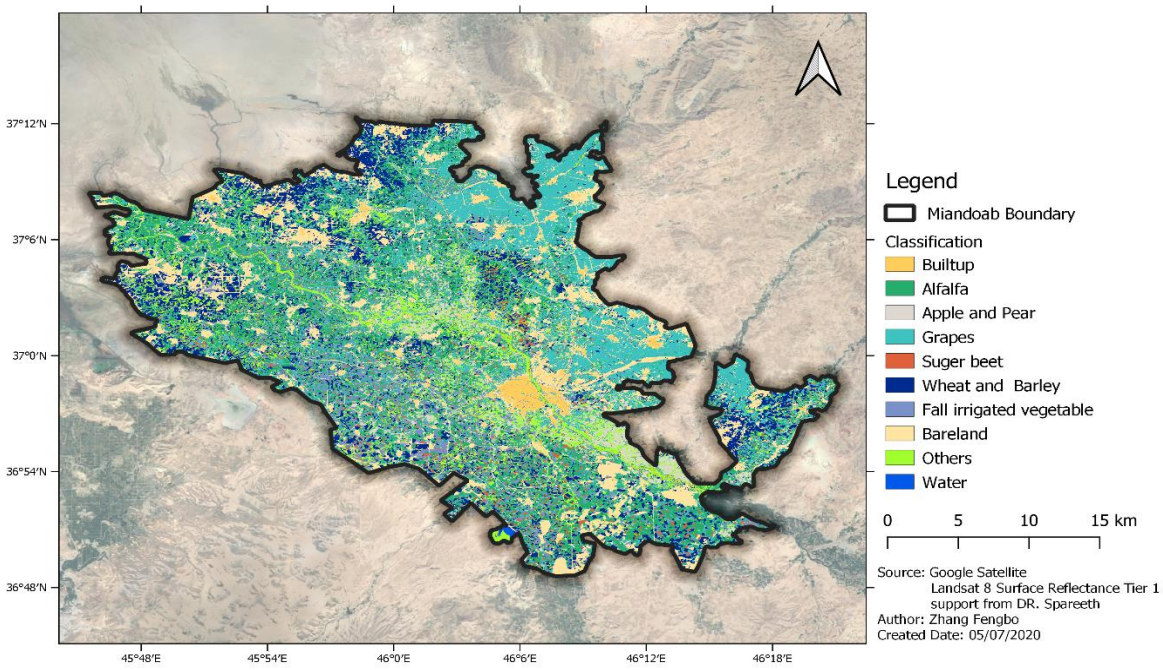

Figure 11 Crop type map using Landsat 8

The crop type map using Landsat 8 is shown in fig.11 with apparently increasing Others area, compared with the map using Sentinel ½. More directly pieces of evidence shown in table 4 that the area of Bareland, Others and Fall irrigated vegetable grows in varying degrees with 193.7 km2, 106.3 km2 and 96.7 km2, while the area of other land cover decrease. According to the accuracy assessment, accuracy of the classification using Landsat 8 is less than the results selected Sentinel ½, which overall accuracy and kappa statistic are 79% and 0.73 respectively. Importantly, the pixel values of images from Landsat 8 for identifying Apple and Pear is bad with producer accuracy of 36%.

Table 4 Area of land cover using Landsat 8

Class_id	Land Cover(use)	Area(km2)
1	Builtup	20.5
2	Alfalfa	204.9
3	Apple and Pear	52.1
4	Grapes	246.2
5	Sugar beet	23.8
6	Wheat and Barley	157.4
7	Fall irrigated vegetable	96.7
8	Bareland	193.7
9	Others	106.3
10	Water	1.1

Table 5 Accuracy of classification using Landsat 8

Class_id	Crop type	User's accuracy	Producer accuracy
1	Builtup	93%	100%
2	Alfalfa	59%	85%
3	Apple and Pear	50%	36%
4	Grapes	93%	97%
5	Sugar beet	69%	79%
6	Wheat and Barley	80%	67%
7	Fall irrigated vegetable	64%	62%
8	Bareland	87%	93%
9	Others	55%	37%
10	Water	100%	100%
Overall accuracy		79%	
Kappa		0.73	

4.4.2 Effect of different algorithms

Not all of supervised machine learning algorithms are useful for classification in Miandoab. For exploring the influence of algorithms on the accuracy of the crop type map, the CART test was chosen. Apparently, the results of estimation and classification in areas of Sugar beet and Apple and Pear are bad due to low user's accuracy and producer accuracy, which is under 50%, as shown in table 6.

Table 6 Accuracy of classification by CART algorithm

Class_id	Crop type	User's accuracy	Producer accuracy
1	Builtup	88%	100%
2	Alfalfa	59%	65%
3	Apple and Pear	45%	64%
4	Grapes	96%	91%
5	Sugar beet	31%	36%
6	Wheat and Barley	57%	67%
7	Fall irrigated vegetable	64%	54%
8	Bareland	86%	86%
9	Others	46%	37%
10	Water	100%	100%
Overall accuracy		72%	
Kappa		66%	

5. Discussion

5.1 A bug in pre-processing images from Landsat 8 in GEE

When we directly ran the script using the images from Landsat 8 in GEE, Bulitup area disappeared, and the system did not calculate the accuracy in that area. The reason is that the reflectance recording from Landsat 8 in the urban area in season 1 is too small, which the urban areas are cancelled as clouds by clouds-optimal script. In my opinion, the way fixed this bug is directly deleting the clouds-optimal code and running script again.

5.2 Reliable of accuracy assessment

Indeed, the results of accuracy assessment are very nice with a high overall accuracy of 85% and Kappa statistic of 0.82, even user's accuracy and producer accuracy of both 100% in the classification of Water. However, is it true? The crop type map presents clearly that the green line with red arrow, which was identified to 'Others' is the river obviously, as shown in figure 10. Therefore, there still have huge errors in land cover classification. The ideal way to fix this problem is increasing the number of ground-truth data and evenly distribution in the study area, especial the number of data for water identification. But this method is a bit unrealistic due to the limitation of funds and expensive in-situ measurement. Thus, we should focus on improving the methodology in classification, increasing the resolution of input data and other ways of enhancing accuracy.

5.3 Effect of input satellite data

With the RS technique developing, the resolution of the satellite data has risen. In this case, Sentinel ½ is selected as the input data source. The ground spatial resolution of images from Sentinel 2 is 10 m for the band 2,3,4,8 in the visible and near-infrared, and 20 m for band 5, 6, 7, 8a, 11, 12 in visible and shortwave infrared, while the resolution of images from Landsat 8 is 30 m. Thus, the accuracy of crop type map using Sentinel data is apparently higher than the accuracy using Landsat data. Especially, the pixel values of images from Landsat 8 for identifying Apple and Pear is very bad with producer accuracy of 36%. Moreover, the reason for the low resolution of the image from Landsat 8 is the technical limitation when the satellite was launched in 2013. And Sentinel 2 was launch in 2017.

5.4 Effect of different algorithms

Not all of supervised machine learning algorithms are useful for classification in Miandoab. For exploring the influence of algorithms on the accuracy of the crop type map, the CART test was chosen. Apparently, the results of estimation and classification in areas of Sugar beet and Apple and Pear are bad due to low user's accuracy and producer accuracy, which are under 50%, as shown in table 6. In my opinion, the more suitable algorithm in this research area is Random Forest test, and we need to try more methods to improve the classification accuracy.

Reference

1. Alpaydin, E. (2020), *Introduction to machine learning*, MIT press.
2. Fang, H. (1998), Rice crop area estimation of an administrative division in China using remote sensing data, *International Journal of Remote Sensing*, *19*(17), 3411-3419.
3. Faramarzi, N. (2012), Agricultural water use in Lake Urmia basin, Iran: An approach to adaptive policies and transition to sustainable irrigation water use, edited.
4. Gallego, F. J. (2004), Remote sensing and land cover area estimation, *International Journal of Remote Sensing*, *25*(15), 3019-3047.
5. Hesami, A., and A. Amini (2016), Changes in irrigated land and agricultural water use in the Lake Urmia basin, *Lake and Reservoir Management*, *32*(3), 288-296.
6. JICA (2016), Data collection survey on hydrological cycle of Lake Urmia basin in the Islamic Republic of Iran.
7. Joseph, G. (2005), *Fundamentals of remote sensing*, Universities Press.
8. Lewis, H., and M. Brown (2001), A generalized confusion matrix for assessing area estimates from remotely sensed data, *International journal of remote sensing*, *22*(16), 3223-3235.
9. Liaw, A., and M. Wiener (2002), Classification and regression by randomForest, *R news*, *2*(3), 18-22.
10. McHugh, M. L. (2012), Interrater reliability: the kappa statistic, *Biochemia medica: Biochemia medica*, *22*(3), 276-282.
11. Michel, D. (2017), Iran's impending water crisis, *Water, Security and US Foreign Policy*, 168.
12. Schulz, S., et al. (2020), Climate change or irrigated agriculture–what drives the water level decline of Lake Urmia, *Scientific reports*, *10*(1), 1-10.
13. Stehman, S. V. (2009), Model-assisted estimation as a unifying framework for estimating the area of land cover and land-cover change from remote sensing, *Remote Sensing of Environment*, *113*(11), 2455-2462.
14. Tamiminia, H., et al. (2020), Google Earth Engine for geo-big data applications: A meta-analysis and systematic review, *ISPRS Journal of Photogrammetry and Remote Sensing*, *164*, 152-170.